## **Controlling Homogeneous Microrobot Swarms** *In Vivo* Using Rotating Magnetic Dipole Fields

Jake J. Abbott and Henry C. Fu

**Abstract** Future medical microrobots, which are likely to be simple microstructures with no actual computational intelligence on board, can be functionalized to perform targeted therapy in the body. In this paper, we describe how the properties of rotating magnetic dipole fields have the potential to enable *in vivo* swarm control for the popular class of magnetic microrobots that convert rotation into forward propulsion. The methods we describe can be used with swarms of batch-fabricated homogeneous microrobots, and do not require any localization information beyond what is realistically obtainable from medical images.

Biomedical "microrobots", which are typically conceived as simple microstructures with no actual computational intelligence on board, can be functionalized to perform targeted therapy in the body such as chemotherapy or hyperthermia [10, 14]. The majority of the work on biomedical microrobots has focused on magnetic swimmers and screws that use a chiral structure (*e.g.*, a helix) to convert magnetic torque generated by a rotating magnetic field into forward propulsion, although we have shown that achiral structures can also be propelled in the same fashion [3]. This method of propulsion compares favorably to other methods of magnetic propulsion [1].

Biomedical applications will likely require the control of a large number of microrobots (i.e., a swarm) to accomplish a therapeutic task. However, this is difficult for two reasons. First, the entire swarm will be subject to some globally applied magnetic field, and the distances between individual microrobots will be small compared to their distances from the field-generation source, resulting in them experiencing very similar magnetic fields to each other. Second, for clinical use it may be

The authors are with the Department of Mechanical Engineering and Robotics Center, University of Utah, USA. J. J. Abbott is the corresponding author, e-mail: jake.abbott@utah.edu. This work was supported by the National Science Foundation under awards #1435827 and #1650968.

unrealistic to assume that each microrobot can be individually localized; rather, a medical image will show a swarm of microrobots as a blob in the image [13].

To date, research on the control of multiple magnetic microrobots has either considered a small set that are individually localized [5, 6], or a swarm that is controlled as an aggregate unit with no ability to differentiate microrobots [13], or a swarm in which microrobot heterogeneity is required for differentiation [2, 15]. No prior work has proposed a solution for the comprehensive control of a swarm of batch-fabricated homogeneous microrobots, a likely scenario for practical realization.

In this paper, we propose two ways to think about controlling a swarm of homogeneous microrobots *in vivo*. We can treat the swarm as an object to be manipulated, and perform basic manipulation primitives on the swarm such as "move the aggregate swarm to a new location," "spread out the swarm," "gather the swarm together," or "split the swarm into smaller swarms and move them to separate locations." Alternatively, we can directly control the concentration field of the microrobots throughout a volume of interest. We will describe how the unique properties of rotating magnetic dipole fields can be utilized to make both of these strategies possible.

Our group has put significant effort into characterizing and utilizing magnetic dipole fields due to their numerous desirable properties, first and foremost being that they have a simple analytic representation that lends itself to analysis and real-time computation. Dipole fields are generated by spherical permanent magnets, and the fields generated by certain other permanent-magnet geometries and specialized electromagnetic sources can be accurately approximated by the dipole model at clinically realistic distances. It is easy to conceive of a clinical scenario in which the patient is surrounded by one or more relatively small dipole sources in close proximity to the location of interest, as opposed to designing a large one-size-fits-all system into which the patient is placed (which is typical in prior work).

A magnetic dipole moment m generates a field h at each point p (with respect to the dipole), which is described by the point-dipole equation:

$$\boldsymbol{h} = \frac{1}{4\pi \|\boldsymbol{p}\|^3} \left[ 3\hat{\boldsymbol{p}}\hat{\boldsymbol{p}}^T - I \right] \boldsymbol{m} = \frac{1}{4\pi \|\boldsymbol{p}\|^3} H \boldsymbol{m}$$
 (1)

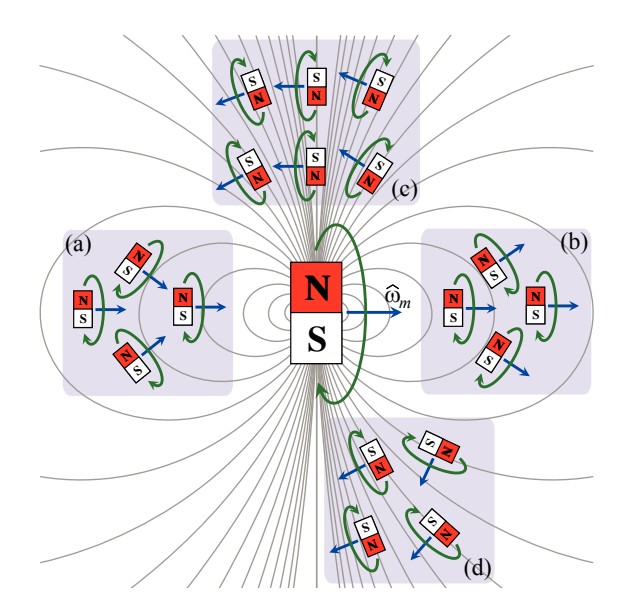
We see that the magnetic field is nonlinear with respect to position, with a strength that decays rapidly from the source as  $\sim \|\boldsymbol{p}\|^{-3}$ , but the field is linear with respect

We have developed a spherical-permanent-magnet robotic end-effector capable of continuous singularity-free rotation of the spherical magnet about any axis [17].

<sup>&</sup>lt;sup>2</sup> We show in [11] that the fields of cubic and certain cylindrical permanent magnets—which are easy to fabricate (and purchase in variety of sizes), fixture, and manipulate—are accurately approximated by the dipole model not far outside of their minimum bounding sphere.

<sup>&</sup>lt;sup>3</sup> We developed an electromagnetic source called the Omnimagnet, comprising three mutually orthogonal coils with a common soft-magnetic spherical core, all in a cubic package [12]. The Omnimagnet was optimized such that its field is accurately approximated by the dipole model just outside of its minimum bounding sphere.

Fig. 1 A magnetic dipole moment m, with instantaneous field lines shown, is rotated about axis  $\hat{\boldsymbol{\omega}}_m$ , with swarms of microrobots shown at different locations. The microrobots are shown simply as rotating magnets without any chiral structure, with their respective  $\hat{\boldsymbol{\omega}}_h$  vectors shown. At locations along the axis of  $\hat{\boldsymbol{\omega}}_m$ , swarms are driven straight while either (a) spreading or (b) gathering the swarm. At a location that is orthogonal to  $\hat{\boldsymbol{\omega}}_m$  such as (c), the swarm does not spread/gather, but it is steered. At general locations, such as shown in (d), the swarm will experience both spreading/gathering and steering.



to the dipole itself. We can use H to capture the shape of the dipole field, which is invariant to distance from the source.<sup>4</sup>

We showed in [8] that if a dipole moment is rotated about, and orthogonal to, some axis  $\hat{\boldsymbol{\omega}}_m$ , then the field at any given point in space will rotate about, and orthogonal to, some axis  $\hat{\boldsymbol{\omega}}_h$ , with the same period. The inverse problem was also solved (i.e., How should we rotate the dipole to achieve some desired  $\hat{\boldsymbol{\omega}}_h$  at some desired location?):

$$\hat{\boldsymbol{\omega}}_h = \widehat{H^{-1}\hat{\boldsymbol{\omega}}_m} \quad \Longleftrightarrow \quad \hat{\boldsymbol{\omega}}_m = \widehat{H\hat{\boldsymbol{\omega}}_h}$$
 (2)

where  $H^{-1} = (H - I)/2$  is always well conditioned. The body of a microrobot located at  $\boldsymbol{p}$  will tend to align with  $\hat{\boldsymbol{\omega}}_h$  as its magnetic element synchronously rotates with  $\boldsymbol{h}$ , and  $\hat{\boldsymbol{\omega}}_h$  will become the microrobot's "forward" direction.

If we consider a swarm of microrobots at some nominal position (e.g., the centroid of the swarm), we observe that each microrobot will be at a different p and will thus experience a different  $\hat{\boldsymbol{o}}_h$ . As shown in Fig. 1, there will be locations in the rotating dipole field in which we can conceive of basic swarm manipulation primitives, such as spreading out or gathering together while moving forward, or steering while moving forward. If the patient is surrounded by multiple sources, or a single moving source, such motions will be possible in arbitrary directions.

The phenomena that we have discussed become less pronounced as we consider locations with increasing distance from the dipole source. It is likely that we will need to utilize nonholonomic control techniques to amplify the phenomena. For

<sup>&</sup>lt;sup>4</sup> We use the "hat" notation to describe unit-normalized vectors (e.g.,  $\hat{\boldsymbol{p}} \equiv \boldsymbol{p}/\|\boldsymbol{p}\|$ ), as well as pointing-direction vectors that are inherently unit length (e.g.,  $\hat{\boldsymbol{\omega}}$ ).

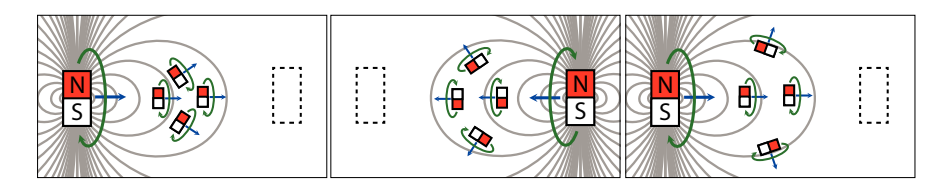


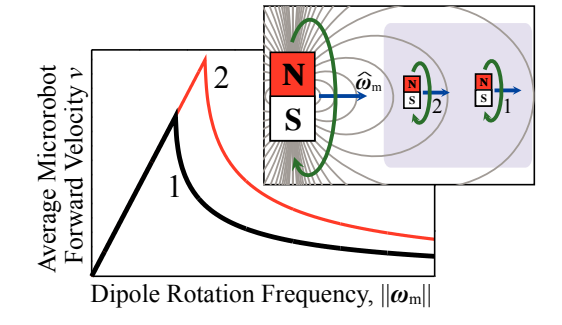
Fig. 2 As the rotating dipole source is alternated (images going from left to right), the swarm can be made to spread out without significant net motion of the centroid.

example, consider the scenario depicted in Fig. 2 in which two dipole sources are on opposite sides of the swarm. By alternating between each source performing the manipulation primitive of Fig. 1(b), the swarm can be made to effectively spread out in place, without a net movement of the centroid. An analogous *gathering* of the swarm can be visualized by considering the microrobots in Fig. 1(a).

Until this point, we have been assuming that all of the microrobots are rotating synchronously with the applied field. However, that need not be the case. Consider the two microrobots swimming along the  $\hat{\boldsymbol{\omega}}_m$  axis in Fig. 1(b). If they are both close enough to the dipole source that the magnetic field is sufficiently strong to keep them both rotating synchronously with the field, then they will move forward at the same average velocity. However, the farther microrobot will be the first to reach the "step-out" regime in which the field is too weak to generate synchronous rotation, at which point the microrobot's average forward velocity will decrease. As shown in Fig. 3, this yields a forward velocity v in the  $\hat{\boldsymbol{\omega}}_h$  direction that transitions between linear and nonlinear dependence on the field rotation frequency  $\|\boldsymbol{\omega}_m\|$  (in general, the forward velocity is a function of both  $\|\boldsymbol{\omega}_m\|$  and  $\boldsymbol{p}$ ). Consider the inset in Fig. 3: this phenomenon will enable the closer microrobot to catch up with the farther, effectively creating another means to gather the swarm. An analogous *spreading* of the swarm can be visualized by considering the microrobots in Fig. 1(a).

A general description of the behavior of a population of microrobots can be constructed as follows. Consider a concentration (density) field of microrobots  $\rho$  at some time. Then, since at each position  $\boldsymbol{p}$ , microrobots move with velocity magnitude v in direction  $\hat{\boldsymbol{\omega}}_h$ , we can interpret  $v\hat{\boldsymbol{\omega}}_h$  as the standard velocity field for micro-

Fig. 3 In [9] we showed how the step-out regime can be exploited to differentiate heterogeneous microrobots in a rotating uniform field. The same concepts can be applied to the homogeneous microrobots in a nonuniform dipole field of interest here. Note: the step-out frequencies are not shown to scale with the microrobot locations depicted.



robots used in continuum fluid mechanics [7]. Therefore, for example, by number conservation the density profile evolves in time as

$$\frac{\partial \rho}{\partial t} = -\nabla \cdot (\rho v \hat{\boldsymbol{a}}_h). \tag{3}$$

This formalism can be directly related to the primitives in Fig. 1. To determine if a local population of microrobots is spreading or gathering, one would examine the rate of change in density *moving with that local population*, *i.e.*, the material derivative of the density:

$$\frac{D\rho}{Dt} \equiv \frac{\partial \rho}{\partial t} + (v\hat{\boldsymbol{\omega}}_h \cdot \nabla)\rho = -\rho \nabla \cdot (v\hat{\boldsymbol{\omega}}_h). \tag{4}$$

A positive/negative value of  $\frac{D\rho}{Dt}$  indicates an increasing/decreasing population concentration and corresponds to gathering/spreading of microrobots. Steering of microrobots is determined by the rate of change of their orientation  $(\hat{\boldsymbol{\omega}}_h)$  moving with the local population:

$$\frac{D\hat{\boldsymbol{\omega}}_{h}}{Dt} \equiv \frac{\partial \hat{\boldsymbol{\omega}}_{h}}{\partial t} + (v\hat{\boldsymbol{\omega}}_{h} \cdot \nabla) \hat{\boldsymbol{\omega}}_{h}. \tag{5}$$

The measures in Eqs. 4 and 5 can be combined to describe all of the scenarios depicted in Fig. 1.

Alternatively, time integration of Eq. 3 suffices to solve the forward problem of how a swarm described by an initial density  $\rho$  would behave for a given time-sequence of dipole strengths and rotation rates, which also enables motion planners that do not rely on primitives. We can conceptualize such a motion planner as follows: (1) Voxelize the given volume, with each of the voxels having a desired concentration of microrobots. From these values, compute the desired centroid and variance of the swarm. (2) Using medical images, estimate the current concentration in each voxel, as well as the current centroid and variance. (3) Construct an objective function that penalizes a combination of the errors in the quantities found in Step 2. This objective function would likely work by driving the centroid and variance of the swarm in the correct direction initially, and then fine-tuning the individual voxel concentrations. (4) For each of the dipole sources, determine the value of  $\hat{\omega}_m$  that would minimize the objective function locally. (5) From the set of  $\hat{\omega}_m$  vectors found in Step 4, choose the one that minimizes the objective function and implement it for a short period of time. (6) Go back to Step 2 and iterate until convergence.

In this paper we have described kinematic models for how rotating dipole fields can be utilized in the control of *in vivo* microrobot swarms. However, we did not model the transient as a microrobot aligns itself with a rapid change in  $\hat{\boldsymbol{\omega}}_h$ , nor did we model other magnetic and fluidic interactions that will certainly exist [4, 16, 18]. In light of this fact, the swarm-manipulation techniques that we have described should be thought of as feedforward models for the purpose of control, and as process models for the purpose of estimation, but with the knowledge that closed-loop feedback of the swarm via medical imaging will be required to ensure the swarm keeps evolving as desired. As we learn more about the unmodeled effects, it may

6 J. J. Abbott and H. C. Fu

be possible to incorporate them into improved kinematic models. Assuming microrobots are not deployed in a flowing environment (e.g., the bloodstream), we anticipate inter-microrobot magnetic interactions to be the most significant disturbance to our model. When might these magnetic interactions ruin our model of control by a dipole field? In typical cases we estimate that a microrobot's magnetic field is comparable to the external field at  $\sim 2$  magnetic-element lengths, i.e., for a quite dense swarm. Although even small magnetic attraction can lead to (irreversible) aggregation, for less dense swarms our methods might be used to prevent such aggregation.

## References

- J. J. Abbott, M. Cosentino Lagomarsino, L. Zhang, L. Dong, and B. J. Nelson. How should microrobots swim? *Int. J. Robotics Research*, 28(11-12):3663–3667, 2009.
- U. K. Cheang, K. Lee, A. A. Julius, and M. J. Kim. Multiple-robot drug delivery strategy through coordinated teams of microswimmers. Applied Physics Letters, 105(8):083705, 2014.
- 3. U. K. Cheang, F. Meshkati, D. Kim, M. J. Kim, and H. C. Fu. Minimal geometric requirements for micropropulsion via magnetic rotation. *Phys. Rev. E*, 90:033007, 2014.
- U. K. Cheang, F. Meshkati, H. Kim, K. Lee, H. C. Fu, and M. J. Kim. Versatile microrobotics using simple modular subunits. *Scientific Reports*, 6:30472, 2016.
- S. Chowdhury, W. Jing, and D. J. Cappelleri. Controlling multiple microrobots: recent progress and future challenges. J. Micro-Bio Robotics, 10(1-4):1–11, 2015.
- 6. E. Diller, J. Giltinan, and M. Sitti. Independent control of multiple magnetic microrobots in three dimensions. *Int. J. Robotics Research*, 32(5):614–631, 2013.
- 7. P. Kunda, I. Cohen, and D. Dowling. Fluid Mechanics. Academic Press, sixth edition, 2015.
- A. W. Mahoney and J. J. Abbott. Generating rotating magnetic fields with a single permanent magnet for propulsion of untethered magnetic devices in a lumen. *IEEE Trans. Robotics*, 30(2):411–420, 2014.
- A. W. Mahoney, N. D. Nelson, K. E. Peyer, B. J. Nelson, and J. J. Abbott. Behavior of rotating magnetic microrobots above the step-out frequency with application to control of multi-microrobot systems. *Applied Physics Letters*, 104(14):144101, 2014.
- B. J. Nelson, I. K. Kaliakatsos, and J. J. Abbott. Microrobots for minimally invasive medicine. *Annual Review of Biomedical Engineering*, 12:55–85, 2010.
- A. J. Petruska and J. J. Abbott. Optimal permanent-magnet geometries for dipole field approximation. *IEEE Trans. Magnetics*, (2):811–819, 2013.
- A. J. Petruska and J. J. Abbott. Omnimagnet: An omnidirectional electromagnet for controlled dipole-field generation. *IEEE Trans. Magnetics*, 50(7):8400810, 2014.
- A. Servant, F. Qiu, M. Mazza, K. Kostarelos, and B. J. Nelson. Controlled in vivo swimming of a swarm of bacteria-like microrobotic flagella. *Advanced Materials*, 27(19):2981–2988, 2015.
- M. Sitti, H. Ceylan, W. Hu, J. Giltinan, M. Turan, S. Yim, and E. Diller. Biomedical applications of untethered mobile milli/microrobots. *Proc. IEEE*, 103(2):205–224, 2015.
- S. Tottori, N. Sugita, R. Kometani, S. Ishihara, and M. Mitsuishi. Selective control method for multiple magnetic helical microrobots. *J. Micro-Nano Mechatronics*, 6(3-4):89–95, 2011.
- S. Tottori, L. Zhang, K. E. Peyer, and B. J. Nelson. Assembly, disassembly, and anomalous propulsion of microscopic helices. *Nano Letters*, 13(9):4263–4268, 2013.
- S. E. Wright, A. W. Mahoney, K. M. Popek, and J. J. Abbott. The spherical-actuator-magnet manipulator: A permanent-magnet robotic end-effector. *IEEE Trans. Robotics*, 33(5):1013– 1024, 2017.
- J. Yu, T. Xu, Z. Lu, C. I. Vong, and L. Zhang. On-demand disassembly of paramagnetic nanoparticle chains for microrobotic cargo delivery. *IEEE Trans. Robotics*, (99):1–13, 2017.